REDVET - Revista electrónica de Veterinaria - ISSN 1695-7504
Vol 25, No.1 (2024)
http://www.veterinaria.org
Article Received: Jan 2024 Revised: Feb 2024 Published: March 2024

Exploring the Potential of TiO_2 Nanoparticles: Optical and Magnetic Properties

S. Rajyalakshmi[1a*], K. Sujatha[2], T.V. Rambabu[3]

[1]Head, Department of Physics, UCST, Adikavi Nannaya University, Rajamahendravaram, AP, India
[2] Principal, VVGIRI Govt Kalasala, Dumpagadapa AKNU
[3] Lecturer in Physics, CSTS Govt. Kalasala, Jangareddigudem AKNU

Corresponding Author: S. Rajyalakshmi
srl.phy@aknu.edu.in

Abstract
Nanoparticles have revolutionized various fields due to their widespread applications in daily life. Among these, semiconducting transition metal oxide Titanium dioxide (TiO2) stands out for its exceptional ultraviolet absorption properties, including antibacterial and photocatalytic activities. TiO2 is an ideal material for preparing organic-inorganic composite materials, existing in both crystalline and amorphous forms. In this study, Titanium dioxide (TiO2) powder was synthesized using the Sol-gel technique, with titanium (4) isopropoxide (TTIP) as the precursor. X-ray diffraction (XRD) analysis confirmed the phase and revealed peaks consistent with the standard spectrum (JCPDS no.: 21-1272 and 21-1276). Scanning electron microscopy (SEM) revealed particle sizes in the nanometer range, with SEM images showing uneven arrangements of nanoparticles with sizes between 55.6 and 68.8 nm. The optical spectra demonstrated enhanced strong and prominent absorption due to the nano size, with a maximum absorption band around 210 nm. Fourier transform infrared spectroscopy (FTIR) recorded at room temperature (4000-400 cm-1) confirmed the presence of functional groups. Electron spin resonance (ESR) spectroscopy revealed the magnetic properties of the sample, with the magnetic resonance field influenced by exchange interaction, resulting in a Dyson line shape and g factor (g = 2).

Key words: XRD, ESR, SEM, Isopropoxide

1. INTRODUCTION

Nanoparticles have become a cornerstone of modern research, with far-reaching applications in various fields, transforming day-to-day life. Titanium dioxide (TiO2) is a versatile material with extensive industrial, environmental, and food-related applications, leveraging its unique properties in dye-sensitized solar cells, sensors, memory devices, photocatalysis, and solar cells [1-5]. TiO2 exists in crystalline and amorphous forms, with three primary crystalline polymorphs: anatase, rutile, and brookite. Anatase and rutile exhibit tetragonal structures, while brookite has an orthorhombic structure [6]. Immobilizing TiO2 nanoparticles on a suitable support has gained traction, as it simplifies phase separation processes and enhances the practicality of these catalysts in industrial settings. Recent studies have demonstrated the photocatalytic activity of immobilized TiO2 particles on microporous ceramic alumina foams [7]. These findings highlight the potential of reticulated macroporous ceramic foams as a promising support for photocatalytic applications and water purification systems. Various methods for preparing TiO2 have been reported, including the hydrolysis of acidic Ti (IV) salt solutions, oxidation of TiCl4 in the gas phase [8-10], and hydrolysis of titanium alkoxides [11, 12]. These approaches yield high-purity TiO2 powders with tailored properties.

2. EXPERIMENTAL SECTION

2.1. Synthesis of TiO2 Nanoparticles via Sol-Gel Technique

TiO2 nanoparticles were successfully synthesized using the sol-gel technique. Titanium (4) isopropoxide (TTIP) served as the precursor, while ethanol and deionized water acted as catalysts.

2.2. Preparation of TiO2 Nanoparticles

A 0.03 molar solution of TTIP was mixed with 0.01 molar deionized water and 20 ml of ethanol. The solution was then stirred at 60°C for two hours under constant stirring to facilitate nucleation and growth of the nanoparticles. Following the reaction, the precipitate was collected via centrifugation and washed twice with acetone and three times with methanol. The sample was then dried under ambient conditions.

2.3. Sintering and Cooling

The dried sample was sintered in a muffle furnace at 120°C for 1 hour, followed by a 2-hour cooling period. The sample was then naturally cooled to room temperature, resulting in the formation of Titanium Oxide.

2.4. Sample Preparation for Further Investigations

The resulting Titanium Oxide was fully ground into a fine powder for further investigations.

REDVET - Revista electrónica de Veterinaria - ISSN 1695-7504
Vol 25, No.1 (2024)
http://www.veterinaria.org
Article Received: Jan 2024 Revised: Feb 2024 Published: March 2024

3. Characterization Techniques

The structural, optical, and morphological properties of the synthesized samples were investigated using various characterization techniques. Powder XRD studies were performed using a Philips PW 1071 diffractometer with Ni-filtered Cu-Kα radiation to determine the crystal structure and lattice parameters. UV-Vis absorption spectra were recorded using a Labindia Analytical UV3092 spectrophotometer to study the optical properties.FTIR spectra were recorded between 500-4000 cm-1 using a Bruker Alpha-T FTIR spectrometer to investigate the functional groups present in the samples. The morphologies and elemental composition of the samples were examined using a Carl Zeiss Supra 55 FE-SEM equipped with an inbuilt EDAX system.

4. RESULTS AND DISCUSSION

4.1. X-ray Diffraction (XRD) Analysis

The structural properties of TiO2 particles were investigated using XRD. The diffractograms were recorded over a 2θ range of 20-70°. Figure 1 presents the representative XRD patterns obtained from the Sol residues. The XRD results revealed the crystalline nature of TiO2, with diffraction peaks corresponding to the rutile and anatase phases of TiO2. The observed peaks showed excellent agreement with the standard spectrum (JCPDS no.: 21-1272 and 21-1276), confirming the presence of both rutile and anatase phases in the synthesized TiO2 particles.

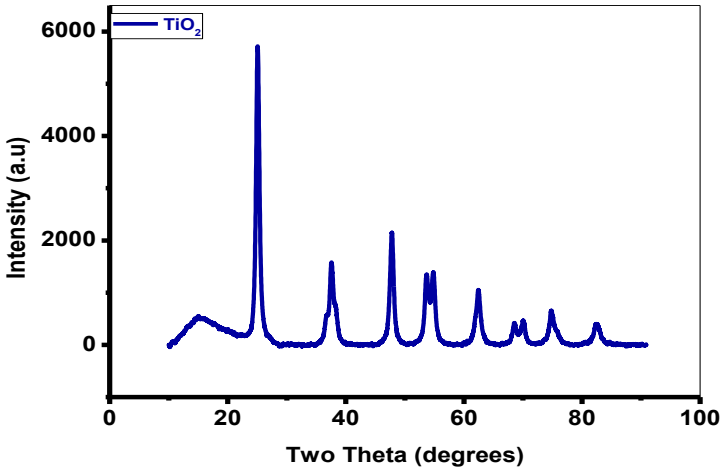

FIGURE 1. XRD patterns of TiO_2.

4.2. UV–vis spectroscopy

4.2.1. Absorption spectrum and optical band gap analysis

The optical properties of the sample were investigated using a LABINDIA UV 3092 UV-Vis Spectrophotometer. The absorbance spectra of the nanoparticles were recorded in the wavelength range of 190-800 nm, using Ethylene glycol as the solvent.Figure 2 presents the absorbance spectrum, which exhibits a strong and prominent absorption band with a maximum absorption peak around 210 nm.The energy band gap was estimated by plotting the absorption coefficient against energy, as shown in Figure 3. The direct band gap was determined to be approximately 4.5 eV.

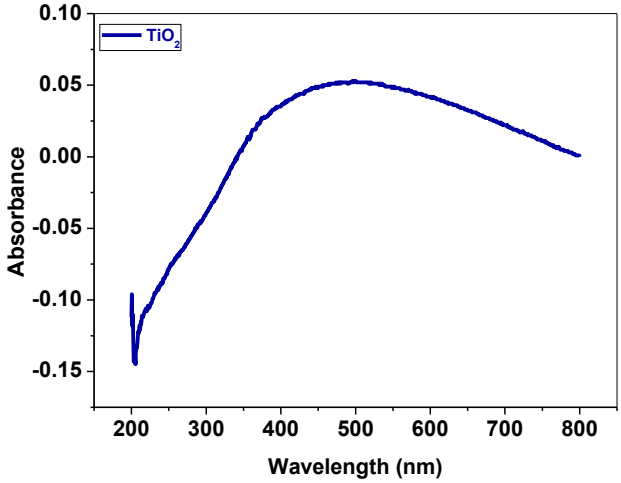

FIGURE 2. UV-Vis Absorbance spectrum of TiO_2

REDVET - Revista electrónica de Veterinaria - ISSN 1695-7504
Vol 25, No.1 (2024)
http://www.veterinaria.org
Article Received: Jan 2024 Revised: Feb 2024 Published: March 2024

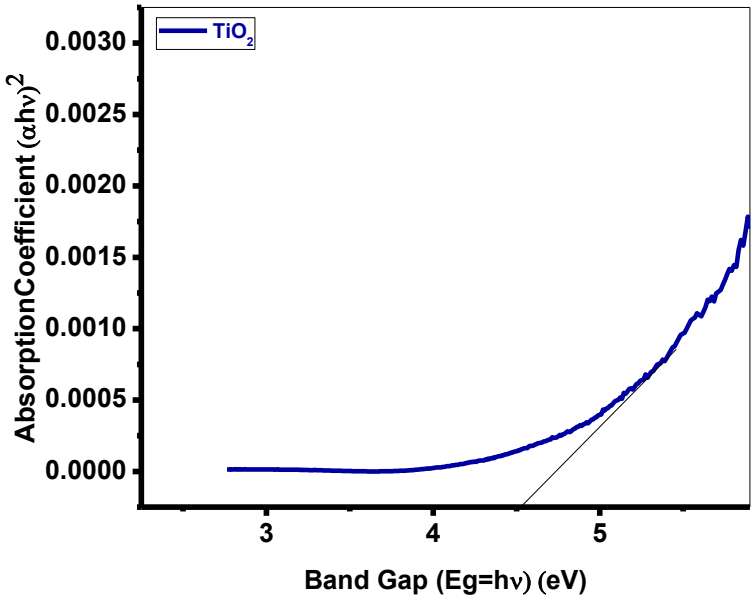

FIGURE 3. Optical Band gaps of pure TiO_2.

4.3. FTIR spectroscopy

Figure 4 presents the Fourier Transform Infrared (FTIR) spectrum of titanium dioxide nanoparticles. The spectrum reveals several distinct peaks. The broad peaks at 3400 and 1631.78 cm-1 are attributed to the stretching and bending vibrations of the hydroxyl (-OH) group. A weak C-H bond stretching peak is observed at 2338 cm-1, while a peak at 1334 cm-1 corresponds to C-H bending vibrations. The peaks in the range of 468-700 cm-1 are assigned to the bending and stretching modes of the Ti-O-Ti bond. Notably, the absence of a peak at 2900 cm-1 indicates that all organic compounds were successfully removed from the samples after calcination [13].

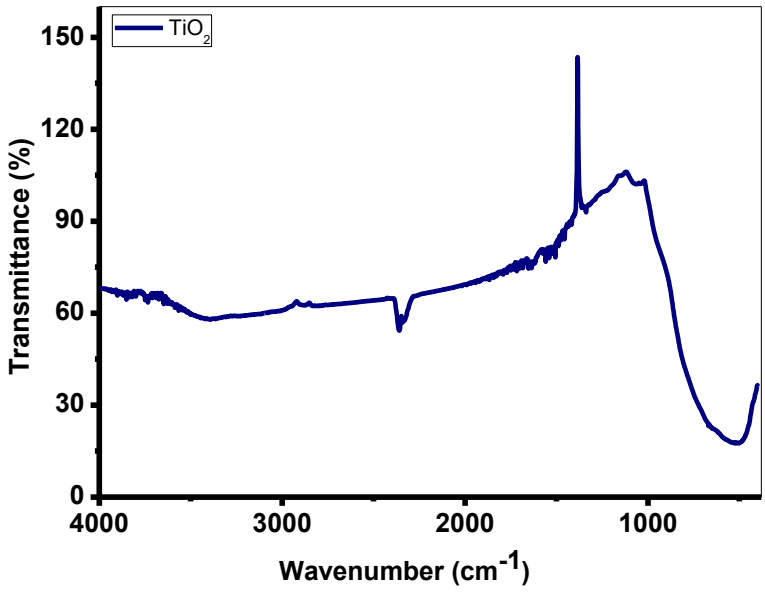

FIGURE 4. FTIR spectra of TiO_2 nano powder.

4.4. SEM with Energy Dispersive X-ray Analysis

Figure 5(a) presents the Scanning Electron Microscope (SEM) image of the TiO2 sample, revealing crystallized particles. The SEM image shows the formation of TiO2 nanoparticles with irregular arrangements, ranging in size from 55.6 to 68.8 nm. This may be attributed to particle agglomeration during the sintering process. The nanoparticles exhibit a roughly spherical, spongy shape. To further confirm the composition, Energy Dispersive X-ray Spectrometry (EDS) was employed. The corresponding EDS spectrum is presented in Figure 5(b), while the quantitative results of the TiO2 nanoparticles are summarized in Figure 5(c).

REDVET - Revista electrónica de Veterinaria - ISSN 1695-7504
Vol 25, No.1 (2024)
http://www.veterinaria.org
Article Received: Jan 2024 Revised: Feb 2024 Published: March 2024

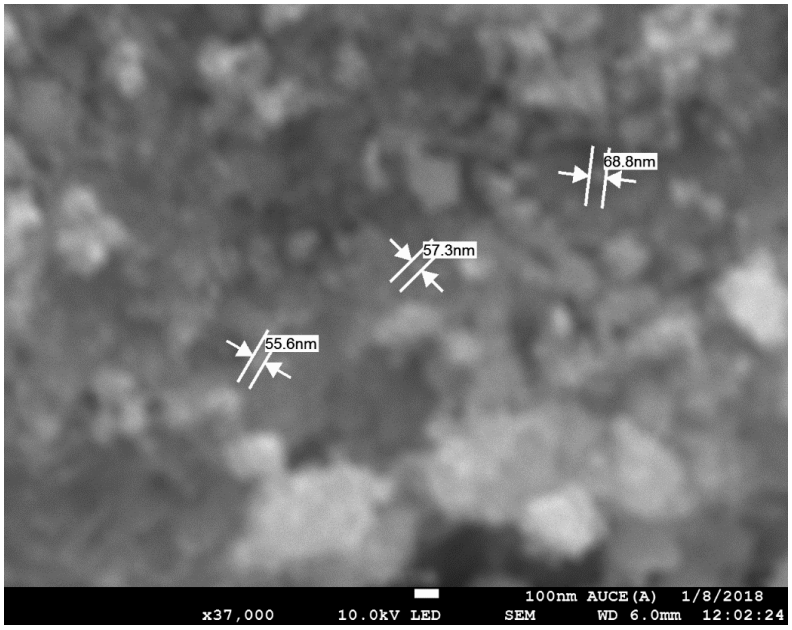

FIGURE 5(a). FE-SEM image of TiO_2 nano particles

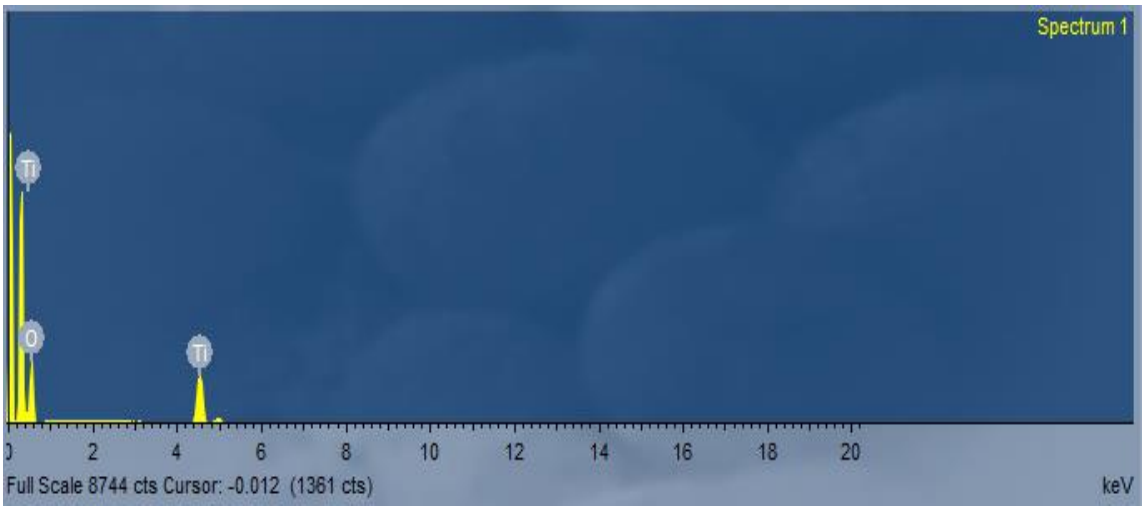

FIGURE 5(b). EDAX spectrum of TiO_2 nano particles.

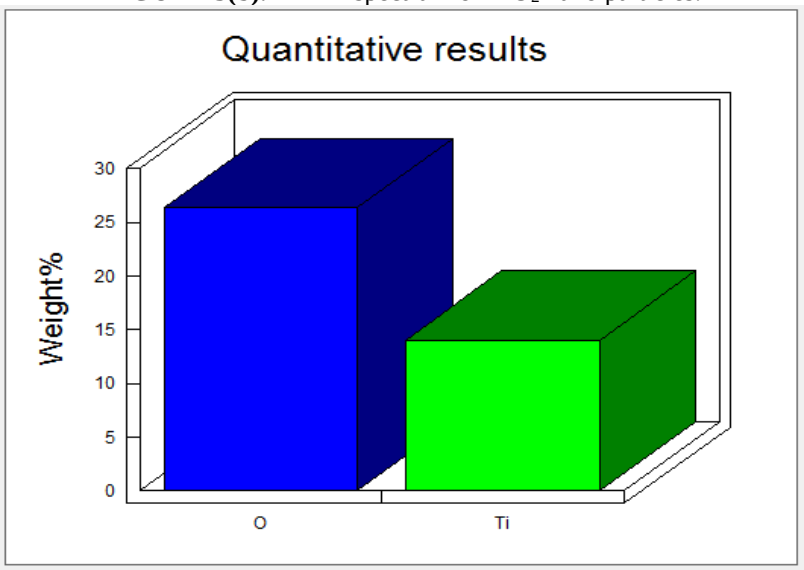

FIGURE 5(c). Quantitative results of TiO_2 nano particles.

REDVET - Revista electrónica de Veterinaria - ISSN 1695-7504
Vol 25, No.1 (2024)
http://www.veterinaria.org
Article Received: Jan 2024 Revised: Feb 2024 Published: March 2024

4.5. Electron Spin Resonance Spectroscopy (ESR)

SR spectroscopy measures the transition frequency between different electron spin states, providing valuable insights into the magnetic properties of materials. In dilute magnetic semiconductors like TiO2, the exchange interaction between free delocalized carriers (holes and electrons) and localized d spins on transition metal ions plays a crucial role in the existence of ferromagnetism. The ESR spectrum of TiO2, depicted in Figure 6, exhibits a Dysonian line shape, indicating a strong exchange interaction between free electrons and localized paramagnetic centers. This interaction is responsible for the room temperature ferromagnetism observed in TiO2. The ESR studies revealed a g-factor of 2, which is consistent with the expected value for TiO2. However, it is worth noting that in certain materials, such as hexagonal ferrites, the g-factor can deviate significantly from 2 and may exhibit anisotropic behavior under specific conditions [14]. The ESR results suggest that the hole-induced ferromagnetism in TiO2 can be interpreted as a diluted magnetic semiconductor.

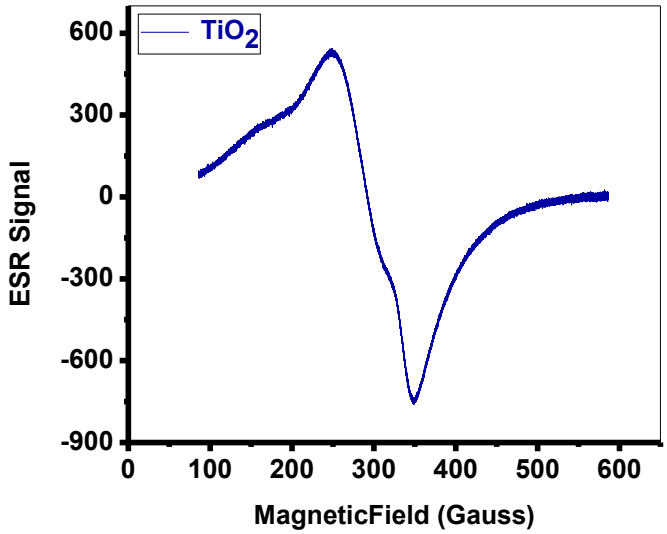

FIGURE 6. ESR Spectra of TiO_2

5. Conclusions

TiO2 nano phosphors were successfully synthesized using the sol-gel technique. The synthesized nanoparticles exhibited a crystalline nature, with X-ray diffraction (XRD) peaks corresponding to the rutile and anatase phases of TiO2. The TiO2 nanoparticles had an average size range of 55.6-68.8 nm. The UV-Vis absorption spectrum showed a prominent peak at 210 nm, indicating a wide band gap of 4.5 eV.Electron Spin Resonance (ESR) studies revealed that the synthesized TiO2 nanoparticles exhibit diluted magnetic semiconductor behavior. The obtained TiO2 nano-powder exhibited excellent optical properties, making it suitable for device applications.

Acknowledgements

The authors express their gratitude towards Dr. K. Vijaya Babu, Andhra University, Visakhapatnam, India for PXRD, ESR, FTIR, UV studies.

References

1. Li, W., Shah, S. I., Huang, C. P., Jung, O., & Ni, C. (2002). Metallorganic chemical vapor deposition and characterization of TiO2 nanoparticles. Materials Science and Engineering: B, 96(3), 247-253.
2. Remillard, J. T., McBride, J. R., Nietering, K. E., Drews, A. R., & Zhang, X. (2000). Real-time in situ spectroscopic ellipsometry studies of the photocatalytic oxidation of stearic acid on titania films. The Journal of Physical Chemistry B, 104(18), 4440-4447.
3. Traversa, E. (1995). Design of ceramic materials for chemical sensors with novel properties. Journal of the American Ceramic Society, 78(10), 2625-2632.
4. O'Regan, B., & Grätzel, M. (1991). A low-cost, high-efficiency solar cell based on dye-sensitized colloidal TiO2 films. Nature, 353(6346), 737-740.
5. Kay, A., & Grätzel, M. (1996). Low-cost photovoltaic modules based on dye-sensitized nanocrystalline titanium dioxide and carbon powder. Solar Energy Materials and Solar Cells, 44(1), 99-117.
6. Mahshid, S., Askari, M., & Ghamsari, M. S. (2007). Synthesis of TiO2 nanoparticles by hydrolysis and peptization of titanium isopropoxide solution. Journal of Materials Processing Technology, 189(1-3), 296-300.

7. Plesch, G., Gorbar, M., Vogt, U. F., Jesenak, K., & Vargova, M. (2009). Reticulated macroporous ceramic foam supported TiO2 for photocatalytic applications. Materials Letters, 63(3-4), 461-463.
8. Formenti, M., Juillet, F., Meriiaudeau, P., Teichner, S. J., & Vergnon, P. J. (1972). Colloid Interface Science, 39, 79.
9. Shi, L. Y., Li, C. Z., & Fang, D. Y. (1998). Materials Review (China), 12, 23.
10. Shi, L., Li, C., Chen, A., Zhu, Y., & Fang, D. (2000). Materials Chemistry and Physics, 66, 51.
11. Mazdiyasni, K. S. (1982). Ceramics International, 8, 42.
12. Yan, M., Rhodes, W., & Sprintger, L. (1982). American Ceramic Society Bulletin, 61, 911.
13. Devi, R. S., Venckatesh, R., & Sivaraj, R. (2014). International Journal of Innovative Research in Science, Engineering and Technology, 3(8), 15206-15211.
14. Zhuravlev, V. A. (1999). Physics of the Solid State, 41, 956-959.